

Journal of Visualized Experiments

In vivo structural assessments of ocular disease in rodent models using optical coherence tomography --Manuscript Draft--

Article Type:	Invited Methods Article - JoVE Produced Video
Manuscript Number:	JoVE61588R1
Full Title:	In vivo structural assessments of ocular disease in rodent models using optical coherence tomography
Section/Category:	JoVE Bioengineering
Keywords:	Optical coherence tomography, retina, retinal degeneration, glaucoma, diabetic retinopathy, myopia, rodent
Corresponding Author:	Rachael Allen Atlanta VA Medical Center Decatur, Georgia UNITED STATES
Corresponding Author's Institution:	Atlanta VA Medical Center
Corresponding Author E-Mail:	restewa@emory.edu
Order of Authors:	Rachael Allen Katie Bales Andrew Feola Machelle T Pardue
Additional Information:	
Question	Response
Please indicate whether this article will be Standard Access or Open Access.	Standard Access (US\$2,400)
Please indicate the city, state/province, and country where this article will be filmed . Please do not use abbreviations.	Decatur, Georgia, USA

TITLE:

In vivo Structural Assessments of Ocular Disease in Rodent Models using Optical Coherence Tomography

AUTHORS AND AFFILIATIONS:

Rachael S. Allen^{1,2}, Katie Bales^{1,3}, Andrew Feola^{1,2}, Machel T. Pardue^{1,2,3}

¹Center of Excellence for Visual and Neurocognitive Rehabilitation, Atlanta Veterans Affairs Medical Center, Decatur, GA

²Department of Biomedical Engineering, Georgia Institute of Technology, Atlanta, GA

³Department of Ophthalmology, Emory University, Atlanta, GA

Email addresses of co-authors:

Katie Bales: klbales@emory.edu

Andrew Feola: andrew.feola@bme.gatech.edu

Machel T. Pardue: machelle.pardue@bme.gatech.edu

Corresponding author:

Rachael Allen, PhD
restewa@emory.edu

KEYWORDS:

Optical coherence tomography, retina, retinal degeneration, glaucoma, diabetic retinopathy, myopia, rodent

SUMMARY:

Here, we describe the use of spectral-domain optical coherence tomography (SD-OCT) to visualize retinal and ocular structures in vivo in models of retinal degeneration, glaucoma, diabetic retinopathy, and myopia.

ABSTRACT:

Spectral-domain optical coherence tomography (SD-OCT) is useful for visualizing retinal and ocular structures in vivo. In research, SD-OCT is a valuable tool to evaluate and characterize changes in a variety of retinal and ocular disease and injury models. In light induced retinal degeneration models, SD-OCT can be used to track thinning of the photoreceptor layer over time. In glaucoma models, SD-OCT can be used to monitor decreased retinal nerve fiber layer and total retinal thickness and to observe optic nerve cupping after inducing ocular hypertension. In diabetic rodents, SD-OCT has helped researchers observe decreased total retinal thickness as well as decreased thickness of specific retinal layers, particularly the retinal nerve fiber layer with disease progression. In mouse models of myopia, SD-OCT can be used to evaluate axial parameters, such as axial length changes. Advantages of SD-OCT include in vivo imaging of ocular structures, the ability to quantitatively track changes in ocular dimensions over time, and its rapid scanning speed and high resolution. Here, we detail the methods of SD-OCT and show examples of its use in our laboratory in models of retinal degeneration, glaucoma, diabetic retinopathy,

and myopia. Methods include anesthesia, SD-OCT imaging, and processing of the images for thickness measurements.

INTRODUCTION:

Spectral-domain optical coherence tomography (SD-OCT) is a precise, high-resolution imaging modality that allows clinicians and researchers to examine ocular structures noninvasively. This imaging technique is based on interferometry to capture three-dimensional retinal images in vivo on a micrometer scale^{1,2}. It has become one of the most frequently used imaging modalities in vision research and in the clinic due to the easy detection and accuracy of pathological features such as structural defects and/or thinning of retinal layers and subretinal fluid³. In research using animal models of vision-related disorders, SD-OCT has provided essential noninvasive analyses of relationships between structure and function and their histopathological origins⁴. Due to its resolution (up to 2-3 microns, depending on the depth into the eye⁵), SD-OCT has the capability to detect even small changes in retinal layer thickness. This type of analysis can provide essential information for disease progression and assess the efficacy of neuroprotective methods and treatments for vision-related disorders.

SD-OCT is a noninvasive alternative to examining structure histologically, and the two have been shown to be correlated⁶. While SD-OCT does not reach cellular resolution, it does allow for longitudinal studies in animals. This is advantageous because disease progression can be tracked in individual animals over time as opposed to having to euthanize animals at specific time points. As imaging techniques continue to improve, SD-OCT technology will also progress, providing enhanced image quality as well as the capability to assess biological processes such as retinal blood vessel function in fine detail. Even since its advent in 1991, SD-OCT technology has seen huge advances in resolution, speed, and sensitivity⁷.

The present study utilizes an SD-OCT system to quantify changes in retinal layers in rodent models of retinal degeneration, glaucoma, and diabetic retinopathy. The SD-OCT system used here is a Fourier-domain OCT-system that utilizes low-power, near-infrared light to acquire, process, and store depth-resolved images in real time. The SD-OCT system has extended depth-imaging capability in the 800 nm wavelength band, providing 8 mm depth and 4 μ m resolution. In Fourier domain detection, the interference signal between scattered light from the tissue and a reference path is Fourier transformed to construct axial scans and/or axial depth profiles of scattered intensity⁸. For the studies here, the OCT beam is scanned over the desired retinal structure while serially acquiring axial scans. Typically, a scan pattern acquires the two-dimensional grid (B-Scans) as a collection of linear one-dimensional scan lines (A-Scans), which correspond to 2D cross-sectional images using a raster scan pattern. For studies focused on myopia in mice, this system is also used to measure dimensions of ocular structures (e.g., cornea thickness, lens thickness, vitreous chamber depth, and axial length).

The current system allows users to design their own protocols, creating scans that can be tailored and selected based on the ocular structures of interest. The principal scans featured in these user defined protocols makes this imaging technique user-friendly. For image analyses, we have developed customized programming in a mathematic modeling program. SD-OCT is a powerful

tool to non-invasively identify and quantify pathomorphological changes in ocular structures and monitor vision-related disease progression.

PROTOCOL:

All procedures described were approved by the Atlanta Veterans Affairs Institutional Animal Care and Use Committee and conformed to the National Institutes of Health guide for the care and use of laboratory animals (NIH Publications, 8th edition, updated 2011).

NOTE: The SD-OCT system used to develop the protocol below is described in the **Table of Materials**. While some of the procedures are specific to this particular system, the overall approach can be adapted for other OCT devices and animal models. Further, in our lab, these protocols are commonly used in mice and rats; however, the overall approach can be adopted to different animal models and SD-OCT devices provided an individual has the correct lens and capabilities on their device.

1. Set up the optical coherence tomography equipment

1.1. Open the SD-OCT software (**Table of Materials**).

1.2. Define who is taking the OCT, the study, and the treatment arm (if relevant). Name these categories in a way that will help researchers search for the desired scans later during data analysis.

1.2.1. In the **Patient/Exam** tab, click **Test Examiner**. Select the name of the examiner. Use the **Setup Examiners & Physicians** button to add new examiners.

1.2.2 Click **Study Name** to define the study. Click the **Study** tab to add a new study or modify treatments in an existing study. Click to the right of **Select Treatment Arm** to select a treatment arm.

1.3 Click the **Add Patient** button, which is used to add a new timepoint for an entire group. When the window appears, enter ID number, First name, and Last name. Select Male or Female. Enter the Date of Birth.

1.4 Click the **Add Exam** button to add the individual rats. To identify the rats, click on an exam. Click **Edit Exam**. Enter the ID number into the **Enter Notes** box. Click the **Save Changes** button.

1.5 Attach the proper lens to the device (**Figure 1B**), select the corresponding Configuration in the software, and dial in the associated reference arm position.

NOTE: The SD-OCT system described has customized lenses, preset scan patterns, and *reference arm* settings specific to the animal species and region of eye being imaged (retina or cornea, mouse or rat). Some of these details are specific to the SD-OCT system described (see table of

materials). For example, not all devices offer manual adjustment of *reference arm* pathlength.

1.6 In the **Patient/Exam** tab, double click the highlighted exam to proceed to the **Imaging** tab and begin imaging or simply click the **Imaging** tab. If there is a default scan, right click to delete it.

1.7 Load a pre-set Scan Protocol by clicking the **Select a protocol from the list** button. Alternatively, add individual scans.

1.8 For rat models of glaucoma and diabetic retinopathy and mouse models of retinal degeneration, choose a pre-set that consists of four images: 2 OD and 2 OS scans. For mouse myopia, choose a pre-set that consists of 8 images: 4 OD and 4 OS scans.

NOTE: Pre-set imaging will be explained in more detail in Section 3. This is something each laboratory makes for themselves or with the manufacturer during on-site installation.

2. Anesthetize the animal

2.1 Administer anesthetic.

2.1.1 Anesthetize rats with ketamine (60 mg/kg) and xylazine (7.5 mg/kg) via intraperitoneal injection.

2.1.2 Anesthetize mice with ketamine (80 mg/kg) and xylazine (16 mg/kg) via intraperitoneal injection.

2.1.3 Wait until animals are fully anesthetized and do not respond to toe pinch.

2.2 Administer pupil dilation drops (1% tropicamide). Wait for pupils to dilate before imaging.

NOTE: Dilation of pupils increases the field of view but is not a requirement. Local (corneal) anesthetic drops (0.5% tetracaine) to numb the eye should also be used if anything will be touching the eye (for example, if applying contact lenses or using a guide). A guide is a device that is placed over the scan head and helps beginners to line up the eye and the scan head.

2.3 After anesthetizing the rodent, place the rodent in a rodent alignment system that can rotate the animal in 3-dimensional space (**Figure 1A, 1C, & 1D**).

NOTE: Currently, we use rodent alignment systems for mice and rats designed and sold with the SD-OCT device.

2.4 Apply liquid (e.g., saline or artificial tears) to keep the eyes lubricated. Ensure that the eye does not dry out during imaging so that the optical properties of the eye are maintained between scans (when the cornea is wet, the retina can be seen clearly).

2.4.1 Make sure to maintain moisture in the opposite eye when scanning the first eye so it does not dry out.

2.5 Use a delicate task wipe to wick away excess saline just before imaging, as too much or too little lubricant on the eye will affect the image quality.

NOTE: Lubricant eye gel can also be used. A contact lens can also be applied to ensure adequate moisture on the eye throughout the test. In our experience a contact lens did not provide a marked improvement in image quality, but contact lenses do help reduce the risk of the cornea drying during the imaging session.

3. Rodent OCT imaging

3.1 Begin with one eye (OS or OD) and image the contralateral eye after.

3.1.1 Position the animal using the two rotational motions of the rodent alignment system, such that the gaze is horizontal and looking down the axis of the OCT Lens (**Figure 1D**).

3.1.2 Use the OCT in Free Run mode to orient the retina for data collection. Use the **Aim** mode (by clicking the **Aim** button) initially for a continuous display of both horizontal and vertical B-scans in real time.

3.1.3 Move the scan head closer to the eye until the retina is visible (as mouse and rat retina lenses are fixed-focus, moving the lens toward the eye focuses deeper into the retina). Then use the rodent alignment system to adjust the animal position up/down and swivel/twist to position the optic nerve head in the center, make the horizontal scan horizontal, and the vertical scan vertical (**Figure 1A**).

3.1.4 Adjust the working distance such that the retinal image is flat and not curved.

3.1.5 Adjust the reference arm position to keep the image near the top of the display window. Be careful not to push in too far or the eye image will flip back on itself.

3.2. Retinal imaging

3.2.1 For glaucoma, retinal degeneration, and diabetic retinopathy models: Define a volume scan that consists of 1000 x 100 x 1 (A scans x B scans x repeated B scans) for averaging. In rats, take a volume scan that is 3 x 3 mm. In mice, take a 1.5 x 1.5 mm volume scan.

3.2.2 Center the optic nerve in the horizontal and the vertical access so that the volume scan is in the center. Take time to make sure the optic nerve head is at the center of the scan and straight along the nasal-temporal and superior-inferior axes (**Figure 2**). Scan and re-center to make sure it is exactly in the center, if needed. Repeat this scan as necessary until the optic nerve head is

centered and aligned along both axes. Click the **Snapshot** button to take a photo.

NOTE: Some SD-OCT devices have the option of optically manipulating the curvature of the eye (e.g., the image is flattened) by adjusting the distance of the eye from the light source with the *reference arm*. We recommend flattening and centering the images when taking direct thickness measurements through the retinal layers to improve accuracy along the anterior-posterior direction.

3.2.3 Click the **Save** button to save the image.

3.2.4 Take a radial scan centered at the optic nerve head that is 1000 x 4 x 20 (A-scan x B-scan x repeated B-scans). Use repeated B scans to enhance image clarity of the eye or retina, which will help to interpret regions of the eye or layers of the retina during data analysis.

NOTE: Again, in rats this radial scan is 3 mm, while in mice the radial scan is 1.5 mm.

3.2.5 Save the image.

3.2.6 Repeat steps 3.1 through 3.2.5 in the contralateral eye.

3.3 Axial length measurements

3.3.1 For projects that involve imaging the whole eye, such as mouse myopia, take three scans of the entire eye and one retina scan for each eye. Choose a pre-set that consists of a radial scan that is 500 x 20 x 1 and encompasses the full diameter of the eye.

NOTE: This setting provides an image of the entire length of the mouse eye from the cornea to the choroid.

3.3.2 Center the middle of the eye and retina in the field of view. Take three radial scans (whole eye scans): a linear B scan that is 1000 x 5 x 2 and two additional linear B scans of 1000 x 5 x 2 at the same location. Save the images.

3.3.3 Afterward, if desired, zoom in and take a volume or rectangular scan (retina scan) similar to the description in 3.2 that consists of 1000 x 20 A scans x B scans. Save the volume scan.

3.3.4 Repeat steps 3.3 through 3.3.3 in the contralateral eye.

NOTE: Axial length measurements are only possible on small eyes (mouse or smaller) since the imaging window of current systems is not large enough to capture a larger eye.

4. Post-imaging steps

4.1 Store saved data on a cloud, which is good practice for data management and allows for easy access for later analysis. Perform data analysis with custom software developed in a mathematical modeling program (**Table of Materials**).

4.2 Remove the rodent from the rodent alignment system and give an intraperitoneal injection of atipamezole (1 mg/kg for rats and mice) to reverse the effects of the xylazine, so that the rodent will wake up more quickly and will be less likely to develop corneal ulcers.

4.3 Allow rodents to recover on a heating pad on low heat. Give additional saline drops as needed. Return rodents to their home cage when they have regained full ambulation.

4.4 Close program and turn off the OCT.

5. Post-processing of OCT images

5.1 Process the images using custom software developed in a mathematical modeling program to suit specific OCT needs (e.g., measure the thickness of areas of interest by manually marking the images).

5.2 Depending on the purpose of the image (mouse retina, rat retina, or myopia/axial length), use one of three different programs:

5.2.1 For processing the retina, select the OCT scans to load. First, define the center of the optic nerve head with a simple click.

5.2.2 Watch as the program generate vertical lines defining distances on either side of the optic nerve head. Note that in the rat retina, these lines are at 0.5 mm and 1.2 mm away from the center of the optic nerve head, for a total of 4 vertical lines representing the nasal-temporal and inferior-superior axes of the eye depending on the radial B scan currently analyzed.

NOTE: In the mouse retina, these vertical lines are at 0.25 mm and 0.5 mm from the optic nerve head center.

5.2.3 Delineate the following layers along each line:

The retinal nerve fiber layer (RNFL), inner plexiform layer (IPL), inner nuclear layer (INL), outer plexiform layer (OPL), outer nuclear layer (ONL), external limiting membrane (ELM), inner segments/outer segments (IS/OS), retinal pigment epithelium (RPE), and total retinal thickness.

NOTE: The radial scan does not typically have nasal/temporal and superior/inferior labels when it is opened. Scans may be created such that they have an n/t and s/i orientation, and those scans in particular are analyzed later.

5.2.4 After an image has been delineated and the program closed, export these measurements into a spreadsheet software for data analysis.

5.3 Use these length and thickness values from step 5 to make comparisons between groups, for example, determining if there are regional differences (n/t/s/i), or longitudinal changes.

5.4 For retinal measurements, first determine if there are any differences in the nasal-temporal and inferior-superior axis at the 0.5 mm and 1.2 mm distances.

NOTE: If differences in quadrants are not observed, the 0.5 mm and 1.2 mm measurements may be averaged together. This is a similar approach for the mouse retinal scans only at 0.25 mm and 0.5 mm.

5.53 For myopia studies, use this program to assess the ocular parameters along the optical axis of the eye. Open the mathematical modeling program. First, select an image to load.

5.3.1 After loading the image, manually mark each scan (radial and B scans). Mark the anterior and posterior edges of the cornea, lens, vitreous chamber, and retina, so that the program will calculate corneal thickness, lens thickness, anterior and vitreous chamber depth, total retinal thickness, total axial length.

5.3.2 After marking, exit the program which prompts a save menu. Save the delineated values in a spreadsheet software and average the three separate scans together.

REPRESENTATIVE RESULTS:

SD-OCT is considered successful if high quality images are obtained such that ocular dimensions can be reliably measured. Here, a variety of uses of SD-OCT are illustrated using models of retinal degeneration, glaucoma, diabetic retinopathy, and myopia.

In a light-induced retinal degeneration (LIRD) model, exposure to bright light (10,000 lux) induces degeneration of photoreceptor cells in the retina⁹. Representative SD-OCT images reveal a thinner outer nuclear layer, which contains the photoreceptor cell bodies, in retinas from LIRD BALB/c mice compared with undamaged (control) mice (**Figure 3A&3B**). After quantifying the retinal layer thickness, a significant difference between undamaged and LIRD mice was observed for total retinal thickness (**Figure 3C**), outer nuclear layer thickness (**Figure 3D**), and IS/OS thickness (**Figure 3E**).

To experimentally model glaucomatous damage, we used a model of ocular hypertension (OHT)¹⁰. In brief, Brown Norway rats (n=35) received an injection of hypertonic saline into the limbus vein of one eye while the contralateral eye served as an internal control¹¹. For glaucoma studies, we quantified retinal nerve fiber layer (RNFL) thickness. After 8 weeks of OHT, we observed distinct remodeling at the optic nerve head, including optic nerve cupping (**Figure 4A&B**). We then quantified RNFL thickness and found RNFL thinning after 8 weeks of OHT compared to baseline measurements (**Figure 4C**).

To model diabetic retinopathy, Goto-Kakizaki rats, a non-obese, polygenic model of diabetes that

develops hyperglycemia as early as 2-3 weeks of age, were used^{12,13}. Retinas from Goto-Kakizaki rats and Wistar rats (non-diabetic controls) were imaged using SD-OCT (**Figure 5A&5B**). At 6 weeks of age, RNFL and total retinal thickness were reduced in Goto-Kakizaki rats compared with Wistar rats in the central retina (data not shown) and the peripheral retina (**Figure 5C&5D**). The greatest differences were observed in the inferior and temporal quadrants of the retina (**Figure 5C&5D**).

To evaluate mouse models for myopia, axial length was measured in *Bmal1*^{-/-} mice. *Bmal1* is a clock gene of interest because circadian rhythms may play a role in myopia development^{14,15}. The axial length of the *Bmal1*^{-/-} mouse eye (**Figure 6B**) is visibly longer than the wild-type eye (**Figure 6A**) in the OCT images. Quantification of the axial length confirms that *Bmal1*^{-/-} mice have significantly longer axial lengths at 84 days of age (**Figure 6C**), showing that the lack of the clock gene contributes to myopia development.

This protocol generated images of ocular structures in models of retinal degeneration, glaucoma, diabetic retinopathy, and myopia. Images were of sufficient quality such that ocular dimensions, including outer nuclear layer, retinal nerve fiber layer, total retinal thickness, and axial length, could be quantified. The results showed that significant differences in the dimensions of ocular structures could be observed in vivo using SD-OCT.

FIGURE AND TABLE LEGENDS:

Figure 1: Setup of SD-OCT equipment. (A) Picture of rodent alignment system and OCT scan head. (B) Picture of rat and mouse OCT lenses. (C) Picture of mouse rodent alignment system illustrating its ability to move in 3-dimensional space. (D) Close up of the rodent alignment system, specifically the knobs that control its movement.

Figure 2: SD-OCT sample scan. Picture of a live scan of the mouse retina just prior to taking a volume or radial scan. (A) depicts the nasal-temporal alignment, while (B) shows the superior-inferior alignment. Once the retinas in these two images are straight in their respective vertical or horizontal planes and the optic nerve is centered in both images, we proceed to acquire the SD-OCT image.

Figure 3: Using SD-OCT to track thinning of the photoreceptor layer over time in a mouse model of retinal degeneration. (A) Representative SD-OCT scan of an undamaged (control) retina from a BALB/c mouse. (B) Representative SD-OCT scan of a retina from a light-induced retinal degeneration (LIRD) BALB/c mouse. (C-E) Quantification of total retinal thickness (C), outer nuclear layer (ONL) thickness (D), and inner segment/outer segment (IS/OS) thickness (E) in undamaged and LIRD Balb/c mice. Mean ± SEM.

Figure 4: Using SD-OCT we measured a decrease in retinal nerve fiber layer thickness and observed optic nerve cupping after inducing ocular hypertension in a rat model of glaucoma. (A) Representative SD-OCT scan of a retina and optic nerve head from a rat eye taken prior to inducing ocular hypertension (Baseline: OHT). (B) SD-OCT scan of the same rat retina after 8-weeks of OHT (experimental model of glaucoma). (C) Quantification of retinal nerve fiber layer

(RNFL) thickness at baseline compared to OHT eyes. Mean \pm SEM. This data has been modified from Feola et al.¹¹

Figure 5: Using SD-OCT to observe decreased total retinal thickness as well as decreased thickness of specific retinal layers in a rat model of diabetes. (A) Representative SD-OCT scan of a retina from a Wistar (Wild-type control) rat. (B) Representative SD-OCT scan of a retina from a Goto-Kakizaki (diabetic) rat. Retinal layers: retinal nerve fiber layer (RNFL), inner plexiform layer (IPL), inner nuclear layer (INL), outer plexiform layer (OPL), outer nuclear layer (ONL), external limiting membrane (ELM), inner segments/outer segments (IS/OS), retinal pigment epithelium (RPE), and total retinal thickness (TRT). (C-D) Quantification of RNFL (C) and total retinal thickness (D) in Wistar and Goto-Kakizaki retinas where the central line is the mean and the shaded area is the SEM for all four quadrants (Sup, Superior; Temp, Temporal; Inf, Inferior; Nas, Nasal) of the peripheral retina (1.2 mm from the optic nerve head). ** $p < 0.01$, *** $p < 0.001$. This figure has been modified from Allen et al.¹³

Figure 6: Using SD-OCT to evaluate axial length in a mouse model of myopia. Whole eye SD-OCT images of wild-type (A) and *Bmal1*^{-/-} (B) mouse eyes at 84 days of age. The eyes of *Bmal1*^{-/-} mice have significantly longer axial length than the wild-type eyes (C). AL: axial length; RT: retinal thickness; VCD: vitreous chamber depth; LT: lens thickness; ACD: anterior chamber depth; CT: corneal thickness. The long vertical line indicates axial length boundaries (top and bottom indicated by horizontal line) for the wild-type eye. Short arrow indicates the posterior axial length marking for the *Bmal1*^{-/-} eye. Mean \pm SEM. The central line down the middle of each image (A&B) is a vertical saturation artifact. It is typically used as a guide to center the eye, but if the scan is well aligned, it can be made to disappear.

DISCUSSION:

High resolution imaging of ocular structures in vivo allows for the assessment of retinal and ocular changes over time. In this protocol, SD-OCT was demonstrated to capture differences in ocular structures in vivo in models of retinal degeneration, glaucoma, diabetic retinopathy, and myopia.

The most critical aspect when performing SD-OCT is obtaining a clear image of the retina or other ocular structure of interest. It is important to take time to make sure the retina is perfectly centered and has excellent clarity. Heavy breathing by the rodent can result in noisy images (the retina can actually be seen to wiggle on screen). This sometimes happens if an animal is not fully unconscious after anesthetic administration. To work around this issue, multiple B scans can be averaged to help visualize where the boundaries of the retinal layers are, and then the best single B scan image can be analyzed.

Another common mistake is that the eye is too dry or too wet. This can be checked easily by applying an additional drop of saline, wicking it away with a laboratory wipe, and assessing whether the image improved in clarity. A consideration to take into account when marking retinal layer thicknesses on SD-OCT images is how to mark the RNFL. While it is possible to differentiate between the RNFL and GCL on some rodent OCTs, often these two layers are indistinguishable. For consistency, we mark the entire RNFL region (RNFL + GCL, when visible) as the RNFL. Some

studies report the RNFL and GCL as separate layers or combine the GCL and inner plexiform layer¹⁶⁻¹⁸, though this research was typically performed in humans, who have much larger eyes than rodents. Reporting of RNFL thickness is more typical in rodent studies^{11,13,19,20}. Another important issue is that very slight changes in marking can cause a very large change, especially in myopia because of the small size of the structures being measured. For example, a 6 μm difference in measurement is equal to a diopter of change in refractive error²¹. Because slight changes make such a big difference in measurement, image clarity is critical.

A limitation of this protocol, and of SD-OCT in general, is that clear ocular media is required for a good image. For example, corneal lesions, lens abnormalities, and cataracts can prevent users from obtaining clear images. This is a problem in diabetic retinopathy imaging, in particular, as cataracts commonly develop in diabetic rodents²². If the cataract or other ocular issue is small, it is sometimes possible to maneuver the scan head around it. For larger ocular media disruptions, retinal OCT images are impossible to obtain. These retinas could still be investigated using histology as retinal histology is not contingent on clear ocular media.

A further limitation is the fact that hyperreflective lesions, such as exudates and hemorrhages, as well as major retinal vessels, result in shadowing of the underlying retinal structures, and thereby details of the underlying morphology are lost. In a case exhibiting choroidal neovascular membrane and diabetic retinopathy/macular edema where the retinal thickness was over 400 μm , it was hard to discern the underlying pathology and choroid²³. Additionally, SD-OCT can only be used to assess thickness at specific locations. SD-OCT also has a limited penetration depth for imaging the choroid and for imaging of whole eyes (the whole eye can be imaged in a mouse, but not in larger animals). Another limitation is that fluorescent or other markers cannot be used with SD-OCT as with scanning laser ophthalmoscopy (SLO). However, typical SLO devices do not allow for the visualization of retinal layers in cross-section with the same ease that is observed with SD-OCT. Finally, the resolution with SD-OCT is not perfect. However, it is much improved over the resolution available at the inception of SD-OCT and continues to improve over time.

In conclusion, the advantages and significance of the SD-OCT technique are that it allows for in vivo imaging of ocular structures and quantitative tracking of changes in ocular dimensions over time, and that it performs this imaging with rapid scanning speed. Because of the high resolution of SD-OCT, it can be used to detect subtle differences that are not observable with the naked eye (**Figures 4 & Figure 5**). Further, SD-OCT is a useful tool to measure multiple parameters of the eye in a number of disease and injury models. In this protocol alone, SD-OCT was used to measure retinal thickness in models of retinal degeneration and diabetic retinopathy, retinal thickness and cupping in a glaucoma model, and axial length in a myopia model. SD-OCT can also be used to measure corneal curvature²⁴, assess retinal changes after blast and traumatic brain injury^{19,25,26}, identify pathology in age-related macular degeneration²⁷, and monitor retinal health during and after ocular injections²⁸ and retinal placement of prosthetic devices like subretinal implants²⁹. It can be used in other animal models such as tree shrews³⁰ and non-human primates³¹ as well. SD-OCT can also be used to localize retinal pathology based on quadrant (superior, inferior, nasal, temporal) and location (central vs. peripheral). The future SD-OCT devices will achieve even

greater resolution. Additionally, OCT angiography is allowing for imaging of the retinal and choroidal microvasculature by utilizing the reflection of laser light off the surface of red blood cells as they move through the retinal vasculature^{32,33}.

ACKNOWLEDGMENTS:

This work was supported by the Department of Veterans Affairs Rehab R&D Service Career Development Awards (CDA-1, RX002111; CDA-2; RX002928) to RSA, Merit Award (RX002615) and Research Career Scientist Award (RX003134) to MTP, Career Development Award (CDA-2, RX002342) to AJF, EY028859 to MTP, NEI Core Grant P30EY006360, Research to Prevent Blindness, and Foundation Fighting Blindness.

DISCLOSURES:

The authors have nothing to disclose.

REFERENCES

- 1 Wojtkowski, M. et al. Ultrahigh-resolution, high-speed, Fourier domain optical coherence tomography and methods for dispersion compensation. *Optics Express*. **12** (11), 2404-2422 (2004).
- 2 Nassif, N. et al. In vivo high-resolution video-rate spectral-domain optical coherence tomography of the human retina and optic nerve. *Optics Express*. **12** (3), 367-376 (2004).
- 3 Theelen, T., Teussink, M. M. Inspection of the Human Retina by Optical Coherence Tomography. *Methods in Molecular Biology*. **1715** 351-358 (2018).
- 4 Nakazawa, M., Hara, A., Ishiguro, S. I. Optical Coherence Tomography of Animal Models of Retinitis Pigmentosa: From Animal Studies to Clinical Applications. *Biomed Research International*. **2019**, 8276140 (2019).
- 5 Drexler, W. et al. Ultrahigh-resolution ophthalmic optical coherence tomography. *Nature Medicine*. **7** (4), 502-507 (2001).
- 6 VanLeeuwen, J. E. et al. Altered AMPA receptor expression with treadmill exercise in the 1-methyl-4-phenyl-1,2,3,6-tetrahydropyridine-lesioned mouse model of basal ganglia injury. *Journal of Neuroscience Research*. **88** (3), 650-668 (2010).
- 7 Tian, J. et al. Performance evaluation of automated segmentation software on optical coherence tomography volume data. *Journal of Biophotonics*. **9** (5), 478-489 (2016).
- 8 Kraus, M. F. et al. Motion correction in optical coherence tomography volumes on a per A-scan basis using orthogonal scan patterns. *Biomedical Optics Express*. **3** (6), 1182-1199 (2012).
- 9 Boatright, J. H. et al. Tool from ancient pharmacopoeia prevents vision loss. *Molecular Vision*. **12** 1706-1714 (2006).
- 10 Morrison, J. C. et al. A rat model of chronic pressure-induced optic nerve damage. *Experimental Eye Research*. **64** (1), 85-96 (1997).
- 11 Feola, A. J. et al. Menopause exacerbates visual dysfunction in experimental glaucoma. *Experimental Eye Research*. **186**, 107706 (2019).
- 12 Goto, Y., Kakizaki, M., Masaki, N. Production of spontaneous diabetic rats by repetition of selective breeding. *The Tohoku Journal of Experimental Medicine*. **119** (1), 85-90 (1976).
- 13 Allen, R. S. et al. Retinal Deficits Precede Cognitive and Motor Deficits in a Rat Model of Type II Diabetes. *Investigative Ophthalmology & Visual Science*. **60** (1), 123-133 (2019).

528 14 Stone, R. A. et al. Altered ocular parameters from circadian clock gene disruptions. *PLoS*
529 *One*. **14** (6), e0217111 (2019).

530 15 Chakraborty, R. et al. Circadian rhythms, refractive development, and myopia.
531 *Ophthalmic & Physiological Optics*. **38** (3), 217-245 (2018).

532 16 Davies, E. C. et al. Retinal ganglion cell layer volumetric assessment by spectral-domain
533 optical coherence tomography in multiple sclerosis: application of a high-precision manual
534 estimation technique. *Journal of Neuro-ophthalmology*. **31** (3), 260-264 (2011).

535 17 Carnevali, A. et al. Optical coherence tomography angiography analysis of retinal vascular
536 plexuses and choriocapillaris in patients with type 1 diabetes without diabetic retinopathy. *Acta*
537 *Diabetologica*. **54** (7), 695-702 (2017).

538 18 Springelkamp, H. et al. Population-based evaluation of retinal nerve fiber layer, retinal
539 ganglion cell layer, and inner plexiform layer as a diagnostic tool for glaucoma. *Investigative*
540 *Ophthalmology & Visual Science*. **55** (12), 8428-8438 (2014).

541 19 Allen, R. S. et al. Long-Term Functional and Structural Consequences of Primary Blast
542 Overpressure to the Eye. *Journal of Neurotrauma*. **35** (17), 2104-2116 (2018).

543 20 Zhao, D. et al. Age-related changes in the response of retinal structure, function and blood
544 flow to pressure modification in rats. *Scientific Reports*. **8** (1), 2947 (2018).

545 21 Schmucker, C., Schaeffel, F. A paraxial schematic eye model for the growing C57BL/6
546 mouse. *Vision Research*. **44** (16), 1857-1867 (2004).

547 22 Aung, M. H., Kim, M. K., Olson, D. E., Thule, P. M., Pardue, M. T. Early visual deficits in
548 streptozotocin-induced diabetic long evans rats. *Investigative Ophthalmology & Visual Science*.
549 **54** (2), 1370-1377 (2013).

550 23 Puzyeyeva, O. et al. High-Resolution Optical Coherence Tomography Retinal Imaging: A
551 Case Series Illustrating Potential and Limitations. *Journal of Ophthalmology*. **2011**, 764183
552 (2011).

553 24 Liu, A. S. et al. Topography and pachymetry maps for mouse corneas using optical
554 coherence tomography. *Experimental Eye Research*. **190** 107868 (2020).

555 25 Mohan, K., Kecova, H., Hernandez-Merino, E., Kardon, R. H., Harper, M. M. Retinal
556 ganglion cell damage in an experimental rodent model of blast-mediated traumatic brain injury.
557 *Investigative Ophthalmology & Visual Science*. **54** (5), 3440-3450 (2013).

558 26 Harper, M. M. et al. Blast-Mediated Traumatic Brain Injury Exacerbates Retinal Damage
559 and Amyloidosis in the APPswePSEN19e Mouse Model of Alzheimer's Disease. *Investigative*
560 *Ophthalmology Visual Science*. **60** (7), 2716-2725 (2019).

561 27 Zhang, M. et al. Advanced image processing for optical coherence tomographic
562 angiography of macular diseases. *Biomedical Optics Express*. **6** (12), 4661-4675 (2015).

563 28 Muhlriedel, R. et al. Optimized Subretinal Injection Technique for Gene Therapy
564 Approaches. *Methods in Molecular Biology*. **1834** 405-412 (2019).

565 29 Adekunle, A. N. et al. Integration of Perforated Subretinal Prostheses With Retinal Tissue.
566 *Translational Vision Science & Technology*. **4** (4), 5 (2015).

567 30 Sajdak, B. S. et al. Noninvasive imaging of the tree shrew eye: Wavefront analysis and
568 retinal imaging with correlative histology. *Experimental Eye Research*. **185** 107683 (2019).

569 31 Dominik Fischer, M. et al. Detailed functional and structural characterization of a macular
570 lesion in a rhesus macaque. *Documenta Ophthalmologica*. **125** (3), 179-194 (2012).

571 32 Hagag, A. M., Gao, S. S., Jia, Y., Huang, D. Optical coherence tomography angiography:

572 Technical principles and clinical applications in ophthalmology. *Taiwan Journal of*
573 *Ophthalmology*. **7** (3), 115-129 (2017).

574 33 Treister, A. D. et al. Prevalence of Subclinical CNV and Choriocapillaris Nonperfusion in
575 Fellow Eyes of Unilateral Exudative AMD on OCT Angiography. *Translational Vision Science &*
576 *Technology*. **7** (5), 19 (2018).

577

Figure 1

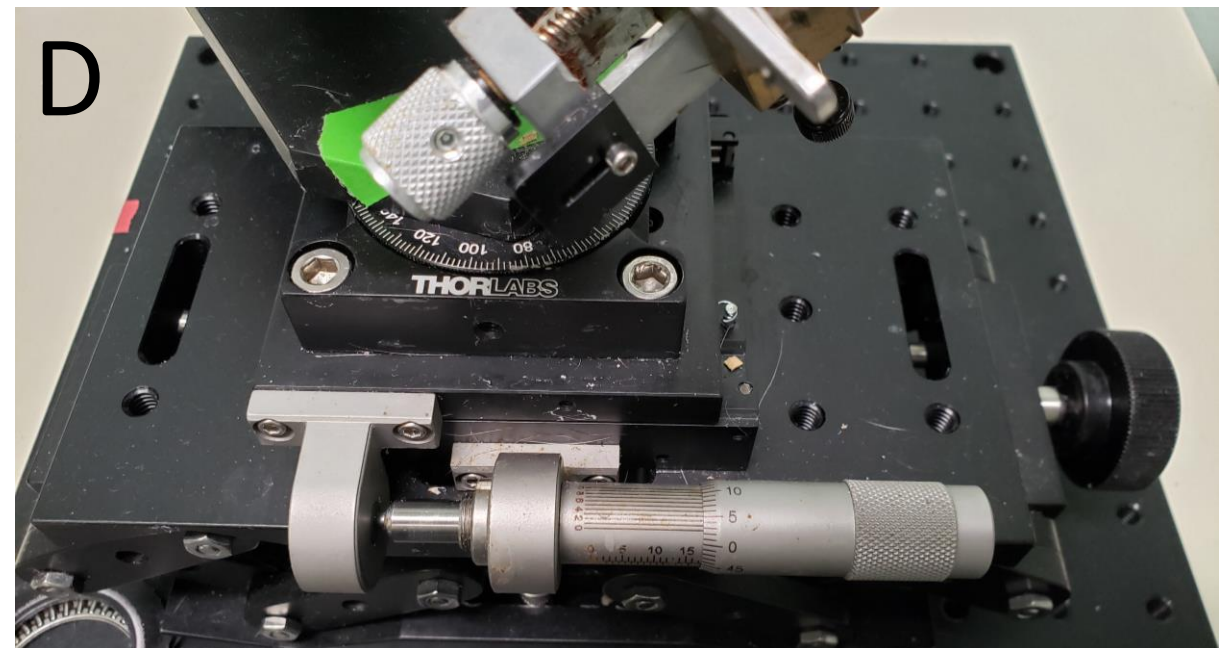
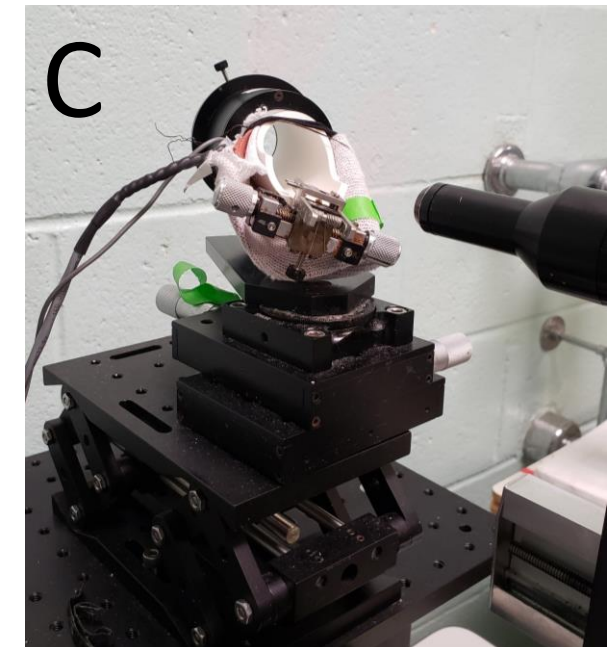
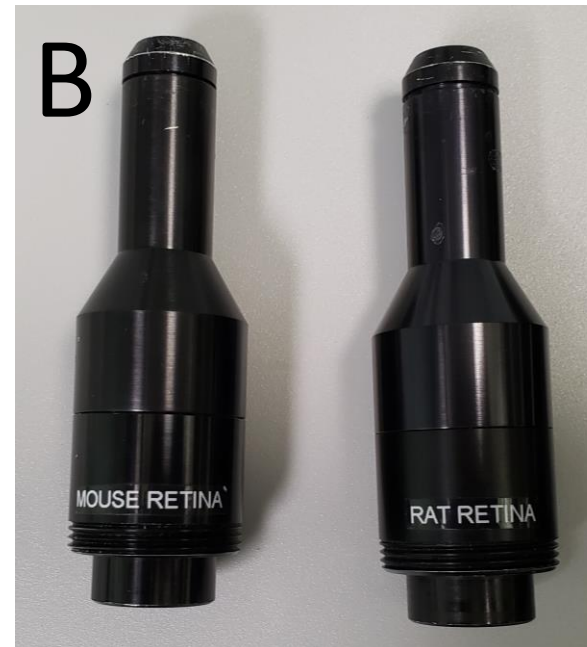
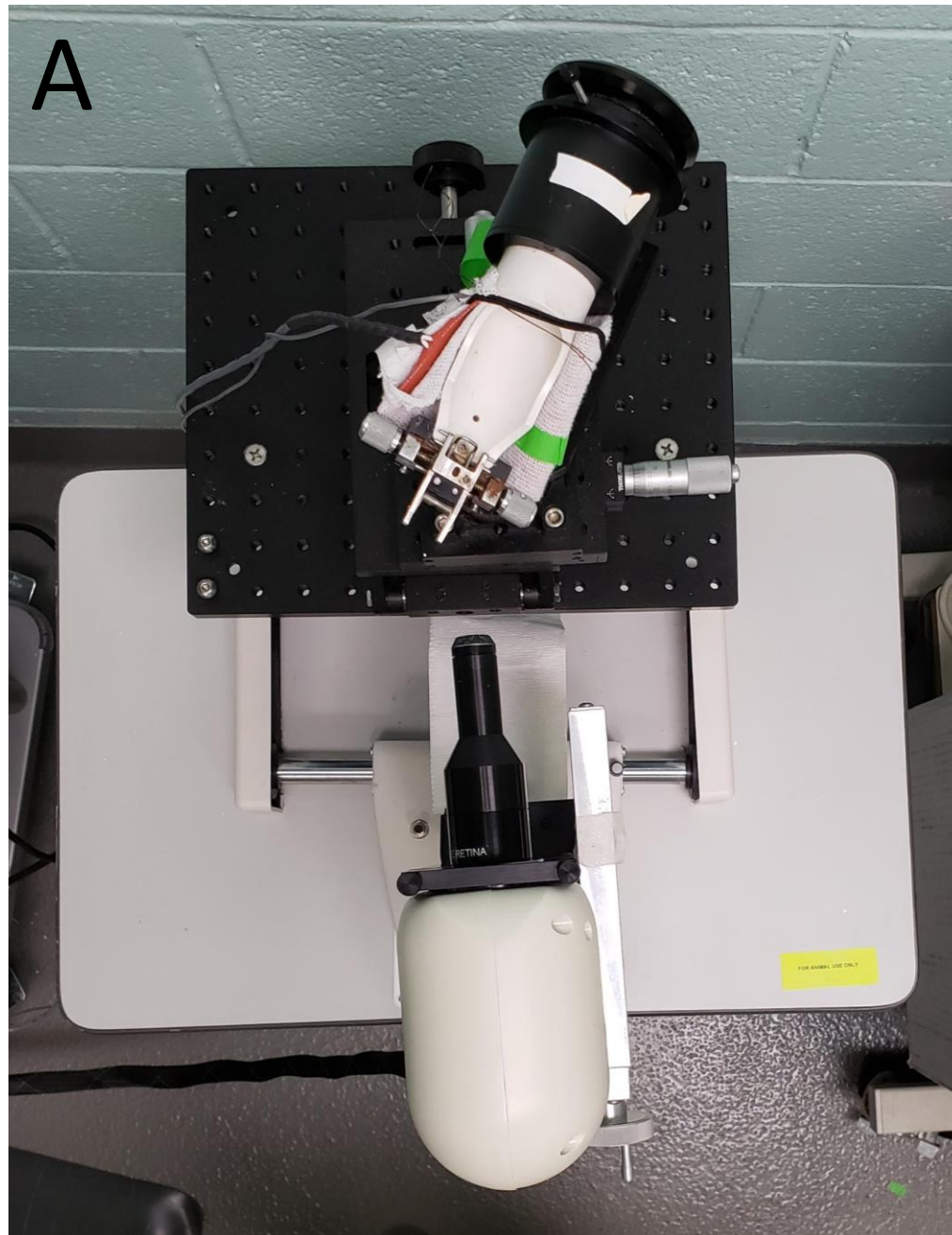
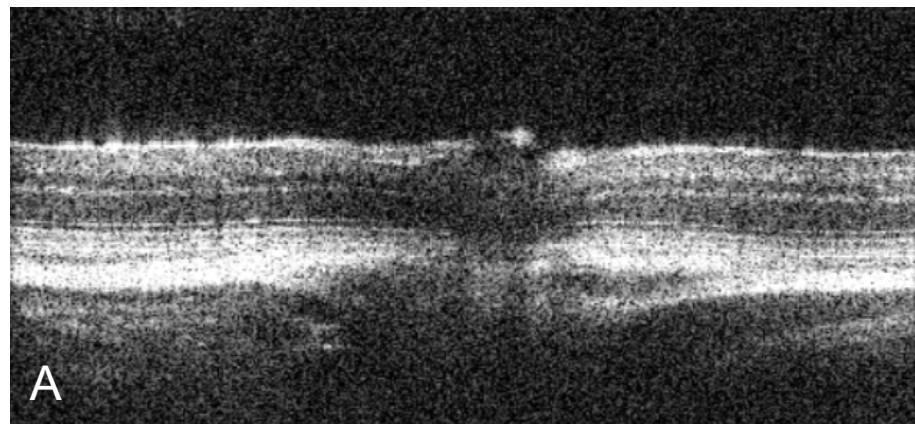


Figure 2

Superior



Temporal

Nasal



B

Inferior

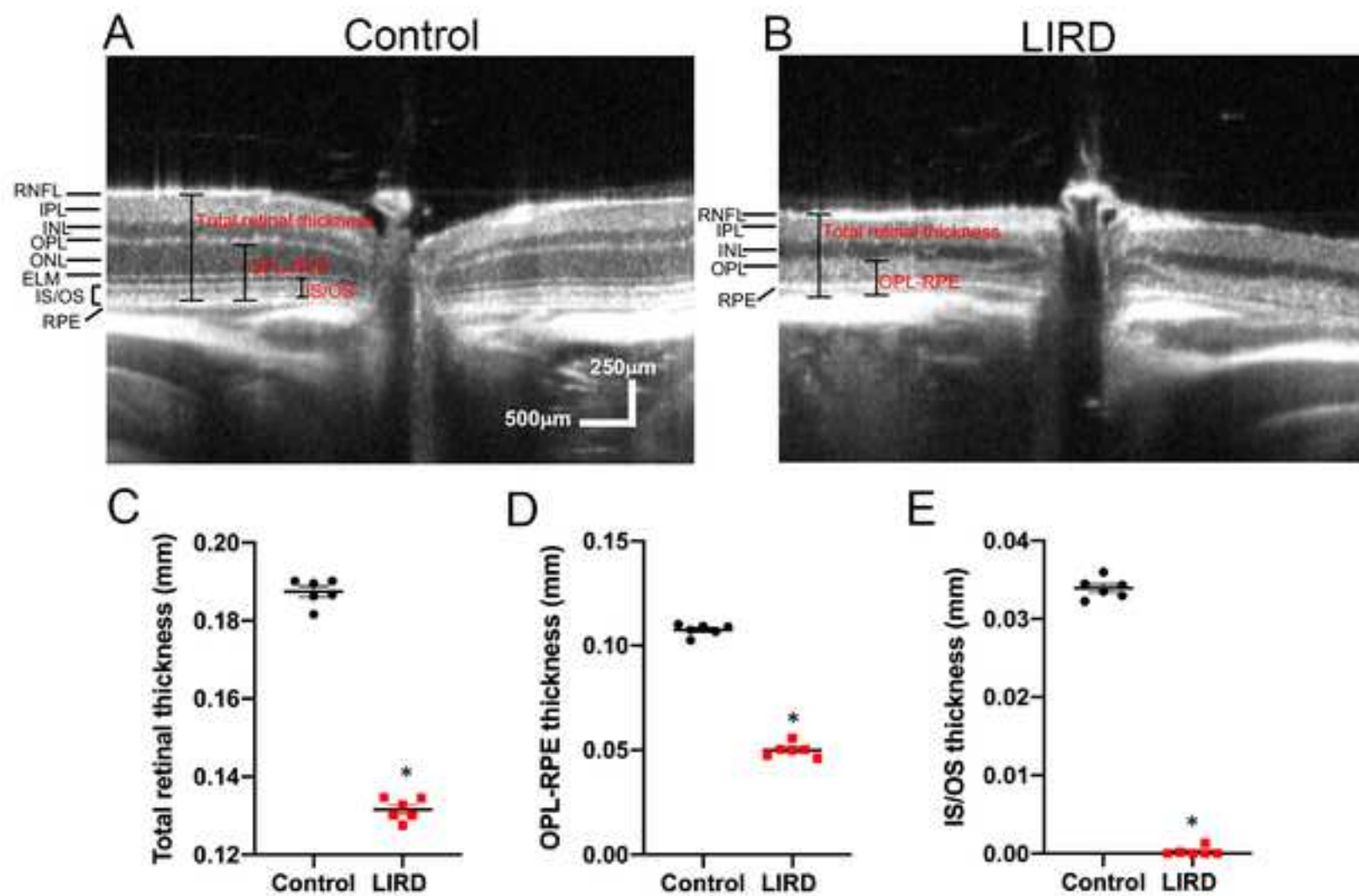


Figure 4

[Click here to access/download;Figure;JoVE OCT fig4.pdf](#)

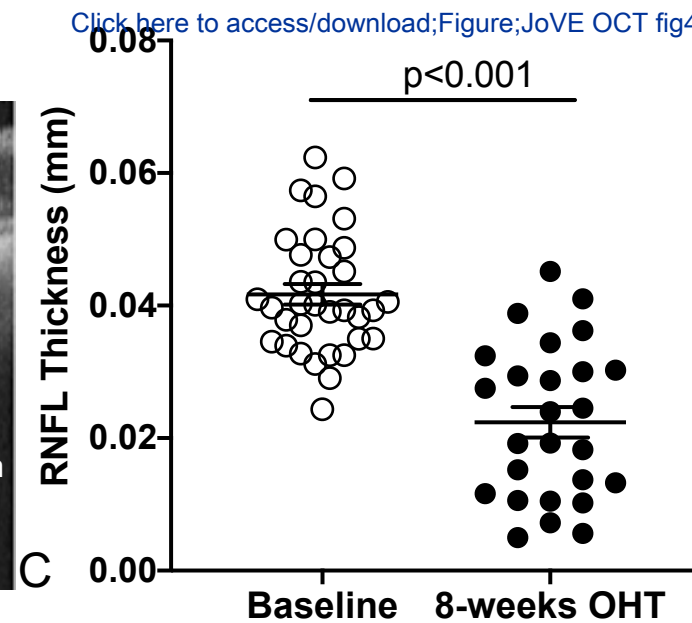
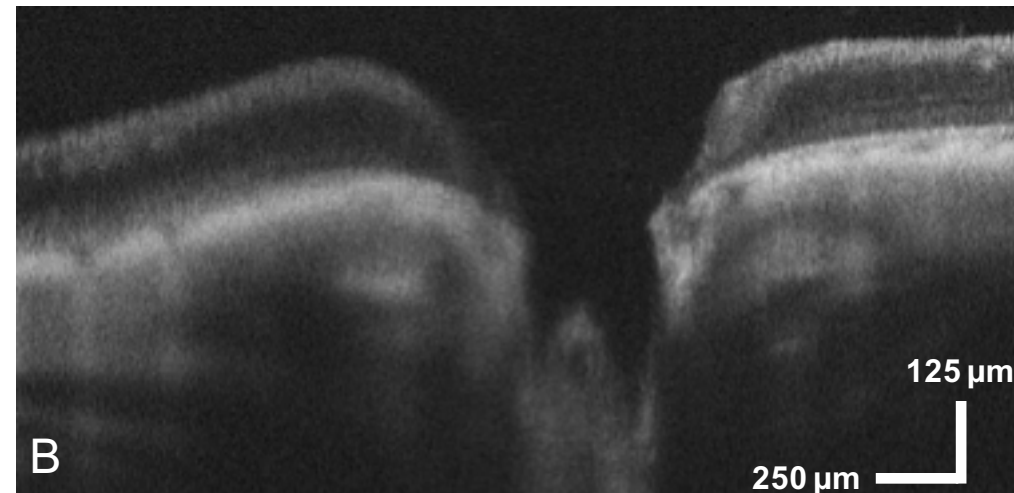
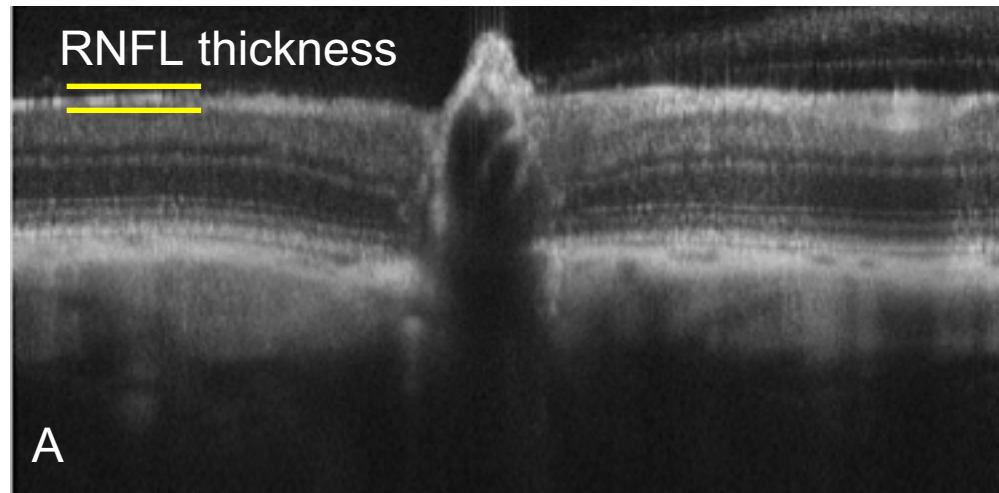
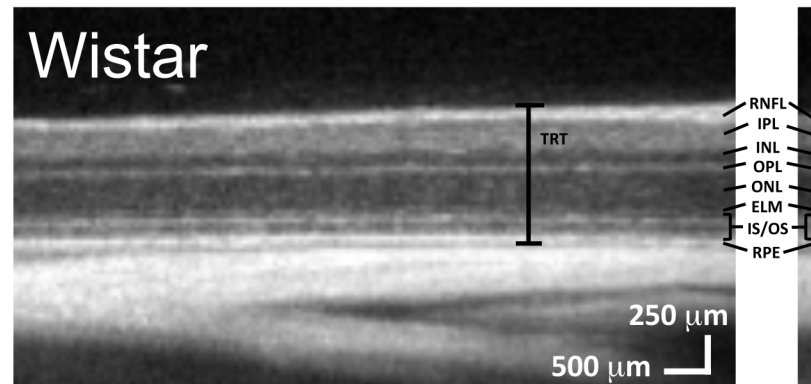


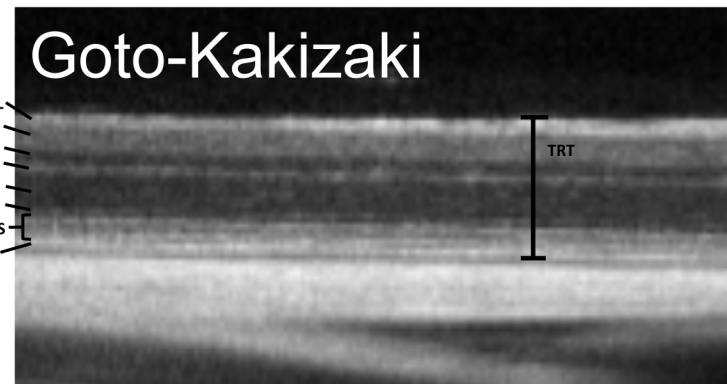
Figure 5

[Click here to access/download;Figure;JoVE Figure 5 final.pdf](#)

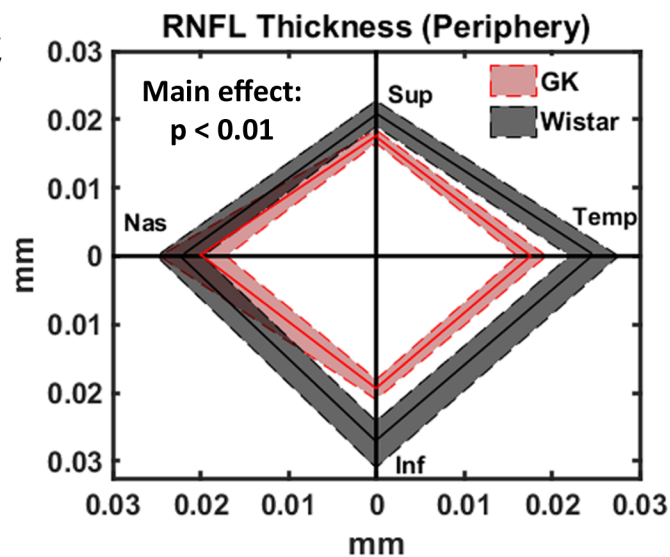
A



B



C



D

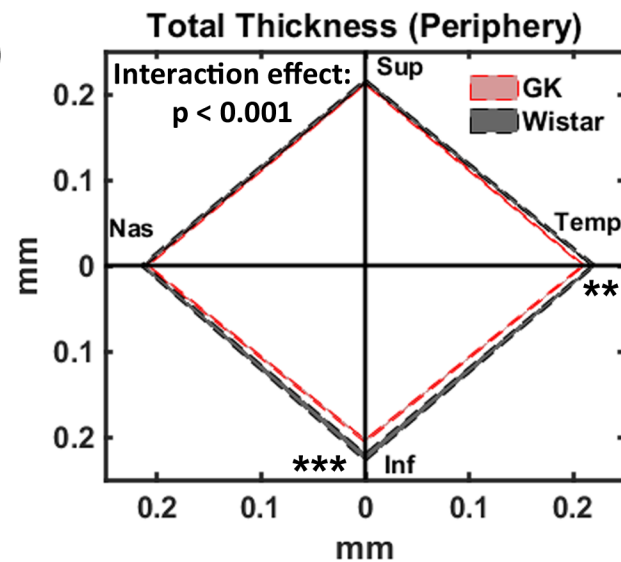
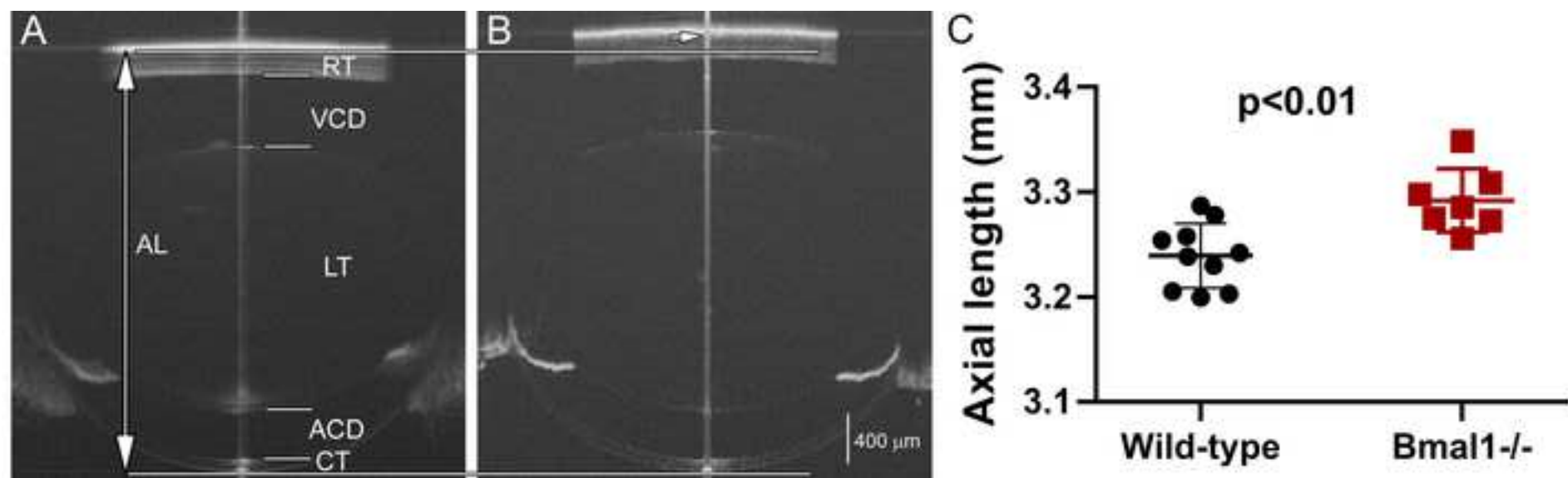


Figure 6



Name of Material/Equipment	Company	Catalog Number	Comments/Description
1% tropicamide	Sandoz	Sandoz #6131403550; NDC- 24208-585-59	
0.5% tetracaine	Alcon	NDC 0065-0741-12	
AIM-RAS G3 120 V	Leica Bioptigen REFRESH	90-AIMRAS-G3-120	Specialized platform to hold the OCT
Celluvisc gel	CELLUVISC	#4554; NDC-0023-4554-30	
G3 18 mm Telecentric Lens	Leica Bioptigen	90-BORE-G3-18	
G3 Mouse Lens	Leica Bioptigen	90-BORE-G3-M	
G3 Rat Lens	Leica Bioptigen	90-BORE-G3-R	
heating pad	Fabrication	11-1130	
InVivoVue software	Leica Bioptigen		Specialized software that pairs with t
MATLAB	Mathworks		mathematical modeling program
Mouse/Rat Kit	Leica Bioptigen	90-KIT-M/R	Mouse/rat rodent alignment system
saline	ADDIPAK	200-39	
System Envisu R4300 VHR 120 V	Leica Bioptigen	90-R4300-V1-120	SD-OCT system

Scanner Head for mice

he Leica Bioptigen SD-OCT system



DEPARTMENT OF VETERANS AFFAIRS
Rehabilitation R&D Service
Center of Excellence for Visual and Neurocognitive Rehabilitation
Atlanta VA Medical Center (151R)
Decatur GA 30033-4004



June 8, 2020

Dear Dr. Jewhurst,

We are very pleased to re-submit our paper, "In vivo structural assessments of ocular disease in rodent models using optical coherence tomography," for publication in the *Journal of Visual Experiments* as part of the methods collection "Three blind mice: methods for assessing retinal and visual disturbances in rodent models."

We thank the editors and reviewers for their insightful comments that have strengthened the manuscript. We are pleased that the reviewers thought the OCT process was described "clearly and comprehensively". We have made the requested revisions to the manuscript based on the editors' and reviewers' suggestions and have addressed the comments in a point-by-point fashion below, with changes throughout the manuscript in tracked changes.

We hope that the manuscript is now acceptable for publication.

Sincerely,

A handwritten signature in black ink that reads "Rachael Allen".

Rachael Allen, PhD
Career Development Awardee (CDA-2)
Atlanta VA Medical Center
Phone: (404)321-6111 x207570; Fax: (404)728-2847
restewa@emory.edu

Editorial Comments:

- Please take this opportunity to thoroughly proofread the manuscript to ensure that there are no spelling or grammatical errors.

Response: Thank you. We have carefully proofread the manuscript for spelling and grammar errors.

• Protocol Language:

1) Please ensure that all text in the protocol section is written in the imperative voice/tense as if you are telling someone how to do the technique (i.e. "Do this", "Measure that" etc.) Any text that cannot be written in the imperative tense may be added as a "Note", however, notes should be used sparingly and actions should be described in the imperative tense wherever possible.

Response: Thank you. We have adjusted all text such that it is written in the imperative voice. We have added any text that cannot be written in the imperative voice as "notes".

2) Split up long steps (3.1) into 2-3 steps.

Response: Thank you. We have split any long steps into multiple steps.

• **Protocol Detail:** Please note that your protocol will be used to generate the script for the video, and must contain everything that you would like shown in the video. **Please add more specific details (e.g. button clicks for software actions, numerical values for settings, etc) to your protocol steps.** There should be enough detail in each step to supplement the actions seen in the video so that viewers can easily replicate the protocol.

Response: Thank you. We have described the protocol in more detail, including button clicks and settings.

• Protocol Highlight:

1) The highlighting must include all relevant details that are required to perform the step. For example, if step 2.5 is highlighted for filming and the details of how to perform the step are given in steps 2.5.1 and 2.5.2, then the sub-steps where the details are provided must be included in the highlighting.

2) The highlighted steps should form a cohesive narrative, that is, there must be a logical flow from one highlighted step to the next.

Response: We have included all relevant details in the highlighted steps. Sometimes we skipped steps because we intend to record the OCT video in rats but not mice. We have worked to ensure the highlighted steps read as a cohesive narrative.

3) Please highlight complete sentences (not parts of sentences). Include sub-headings and spaces when calculating the final highlighted length.

Response: We have highlighted whole sentences and included subheadings and spaces when calculating the final highlighted length.

4) Notes cannot be filmed and should be excluded from highlighting.

Response: Thank you. We have excluded all notes from highlighting.

- **Discussion:** JoVE articles are focused on the methods and the protocol, thus the discussion should be similarly focused. Please ensure that the discussion covers the following in detail and in paragraph form (3-6 paragraphs): 1) modifications and troubleshooting, 2) limitations of the technique, 3) significance with respect to existing methods, 4) future applications and 5) critical steps within the protocol.

Response: We ensured that our discussion has each of these sections. In particular, we have added to our discussion of limitations at the suggestion of one of the reviewers.

- **Figures:** Include scale references for images where appropriate.

Response: Thank you. We have included scale bars on our representative OCT images.

- **References:** Please spell out journal names.

Response: We have spelled out all journal names.

- **Commercial Language:** JoVE is unable to publish manuscripts containing commercial sounding language, including trademark or registered trademark symbols (TM/R) and the mention of company brand names before an instrument or reagent. Examples of commercial sounding language in your manuscript are Bioptigen 4300 SD-OCT system (Leica Microsystems, MATLAB, InVivoVueTM,
1) Please use MS Word's find function (Ctrl+F), to locate and replace all commercial sounding language in your manuscript with generic names that are not company-specific. All commercial products should be sufficiently referenced in the table of materials/reagents. You may use the generic term followed by "(see table of materials)" to draw the readers' attention to specific commercial names.

Response: Thank you. We have changed all mentions of commercial and trademarked materials to generic terms with a note to "see table of materials".

- If your figures and tables are original and not published previously or you have already obtained figure permissions, please ignore this comment. If you are re-using figures from a previous publication, you must obtain explicit permission to re-use the figure from the previous publisher (this can be in the form of a letter from an editor or a link to the editorial policies that allows you to re-publish the figure). Please upload the text of the re-print

permission (may be copied and pasted from an email/website) as a Word document to the Editorial Manager site in the "Supplemental files (as requested by JoVE)" section. Please also cite the figure appropriately in the figure legend, i.e. "This figure has been modified from [citation]."

Response: Thank you. We have uploaded the licensing information.

Reviewer: 1

Manuscript Summary:

The authors described protocol using Bioptigen 4300 SDOCT to acquire data from mice and rats retinas. The authors described the process clearly and comprehensively.

Major Concerns:

I don't have major concerns.

Minor Concerns:

1. In line 191: "1000 x 100 x 1, A scans, B scans, and repeated B scans" is better be written as 1000 x 100 x 1 (A scans x B scans x repeated B scans)
2. Line 234: in -> is
3. Resolution of figure 3 is low.

Response: We thank the reviewer for their careful reading of this manuscript. We have addressed each of these minor concerns.

Reviewer: 2

Manuscript Summary:

The manuscript presents in vivo morphological assessment of ocular structure in normal and diseased rodent models using OCT. It describes several protocols including RNFL thickness, retinal thickness, axial lengths. Generally it is a well written manuscript.

Major Concerns:

None

Minor Concerns:

None

Response: We thank the reviewer for the positive feedback.

Reviewer: 3

Manuscript Summary:

Topic is the use of SD-OCT in visualising ocular structures. Numerous models were interrogated.

Major Concerns:

None

Minor Concerns:

Limitations were not adequately discussed

Response: We thank the reviewer for their feedback. We have added the following to our discussion on limitations: “A further limitation is the fact that hyperreflective lesions, such as exudates and hemorrhages, as well as major retinal vessels, result in shadowing of the underlying retinal structures, and thereby details of the underlying morphology are lost. In a case exhibiting choroidal neovascular membrane and diabetic retinopathy/macular edema where the retinal thickness was over 400 μm , it was hard to discern the underlying pathology and choroid²³. Additionally, SD-OCT can only be used to assess thickness at specific locations. SD-OCT also has a limited penetration depth for imaging the choroid and for imaging of whole eyes (the whole eye can be imaged in a mouse, but not in larger animals).”

Data presented here has been modified from data presented in the following two papers:

Allen, R. S. *et al.* Retinal Deficits Precede Cognitive and Motor Deficits in a Rat Model of Type II Diabetes. *Investigative Ophthalmology & Visual Science*. **60** (1), 123-133, (2019).

Feola, A. J. *et al.* Menopause exacerbates visual dysfunction in experimental glaucoma. *Experimental Eye Research*. **186** 107706, (2019).

Both papers are licensed under a [Creative Commons Attribution 4.0 International License](https://creativecommons.org/licenses/by/4.0/). Link to license information (information from website has also been pasted below):

<https://creativecommons.org/licenses/by/4.0/>

This is a human-readable summary of (and not a substitute for)
the [license](https://creativecommons.org/licenses/by/4.0/). [Disclaimer](#).

You are free to:

- **Share** — copy and redistribute the material in any medium or format
- **Adapt** — remix, transform, and build upon the material
- for any purpose, even commercially.
-



- The licensor cannot revoke these freedoms as long as you follow the license terms.

Under the following terms:

- **Attribution** — You must give [appropriate credit](#), provide a link to the license, and [indicate if changes were made](#). You may do so in any reasonable manner, but not in any way that suggests the licensor endorses you or your use.
- **No additional restrictions** — You may not apply legal terms or [technological measures](#) that legally restrict others from doing anything the license permits.

Notices:

- You do not have to comply with the license for elements of the material in the public domain or where your use is permitted by an applicable [exception or limitation](#).
- No warranties are given. The license may not give you all of the permissions necessary for your intended use. For example, other rights such as [publicity, privacy, or moral rights](#) may limit how you use the material.